Magnesium Borate Nanotubes

Nanotubes of Magnesium Borate

Renzhi Ma, Yoshio Bando, Dmitri Golberg, and Tadao Sato*

Nanoscale tubular structures are currently being researched throughout the world because of their exceptional physical properties and potential applications in nanodevice technology. Since the discovery of carbon nanotubes,[1] there has been active interest in exploring other layered or nonlayered materials that form tubular structures. Successful syntheses of nanotubes based on inorganic binary compounds, such as boron nitride (BN),[2] metal dichalcogenides (i.e., MS_2; M = W, Mo, Nb, Ta, Ti, Zr, Hf,[3a–f] $NiCl_2$[3g]), metal oxides (i.e., VO_x, TiO_2, MoO_3),[4] and organic materials[5] have been reported. Recently, progress was made in the generation of single-crystal tubular structures in a ternary borate system, aluminum borate ($Al_{18}B_4O_{33}$), though the characteristic dimensions were in the micrometer range.[6] This success motivated us to probe the possibility of obtaining intriguing tubular structures based on other metal borates. Besides aluminum borate, magnesium borate is another important ceramic material that has attracted our attention. Magnesium borate was shown to be an interesting thermo-luminescence phosphor.[7] It is also an excellent antiwear, and a reduce-friction additive.[8] Herein, we report the first successful synthesis and characterization of the nanotubular structures of magnesium borate.

[*] Dr. R. Ma, Prof. Y. Bando, Dr. D. Golberg, Dr. T. Sato
Advanced Materials Laboratory
National Institute for Materials Science
Namiki 1-1, Tsukuba, Ibaraki 305-0044 (Japan)
Fax: (+81) 298-51-6280
E-mail: ma.renzhi@nims.go.jp

  DOI: 10.1002/ange.200250455

Magnesium borate nanotubes, approximately 200–500 nm in width, were fabricated by heating a boron thin film coated on a Si(001) wafer with IR radiation in the presence of Mg vapor under an Ar/O_2 atmosphere. Figure 1 shows the scanning electron microscopy (SEM) images of a Si wafer before and after IR irradiation. Figure 1 a depicts the surface morphology of the Si wafer before IR irradiation. Uniform amorphous boron nanoparticles (~50 nm) were homogeneously dispersed on the Si surface. After the IR-irradiation-heating process, the boron nanoparticles on the Si wafer were transformed into totally different nanostructures (Figure 1 b). The more-magnified views (Figure 1 c,d) show that the nanostructures have hollow cores and nanotube morphology. Though a few cylindrical tubes are present, most of the nanotubes appear to have a polyhedral cross-section. Typical widths or diameters of these tubes are 200–500 nm, and lengths vary in the range of 1–5 μm. The nanotubes are usually open at one or both ends; no globules were observed at the tips of these nanotubes.

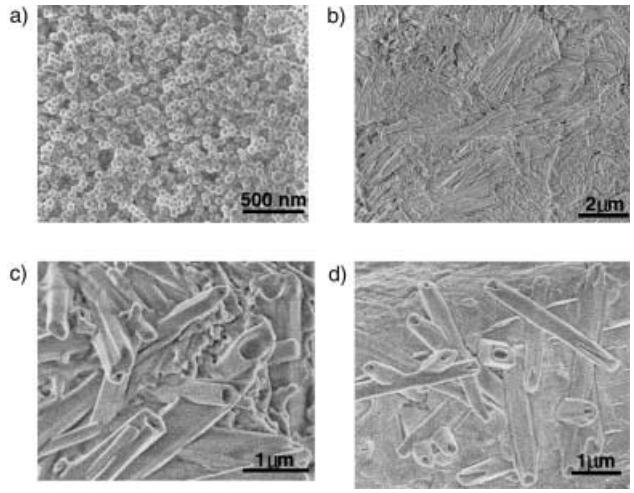

Figure 1. SEM images of surface morphologies of a Si wafer before and after IR irradiation heating. a) Uniform boron nanoparticles before IR heating; (b–d) Nanotube structures formed after IR heating.

During SEM observations, we looked at some regions on the Si wafer surface where the initial nuclei sites for nanotube growth are believed to exist. Figure 2 shows the surface regions with abundant apparent voids. These voids, with dimensions close to cross-sectional dimensions of the hollow nanotubes, may be regarded as the 2D nuclei of the nanotubes.

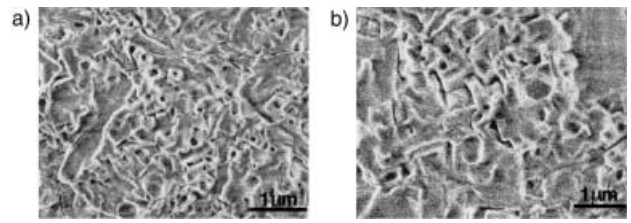

Figure 2. SEM images showing an initial stage of nanotube development. 2D nuclei with hollow cores are apparent.

X-ray diffraction (XRD) measurements of the nanotubes collected from the Si wafer were taken by using a RINT2200 X-ray diffractometer using $Cu_{K\alpha}$ radiation. Figure 3 shows the XRD pattern. All the diffraction peaks can be well indexed to a orthorhombic $Mg_3B_2O_6$ ($3MgO{\cdot}B_2O_3$) phase with the standard lattice constants of $a=5.40$, $b=8.42$, $c=4.50$ Å (JCPDS 38-1475).[9] It thus indicates the nanotubes have the $Mg_3B_2O_6$ structure.

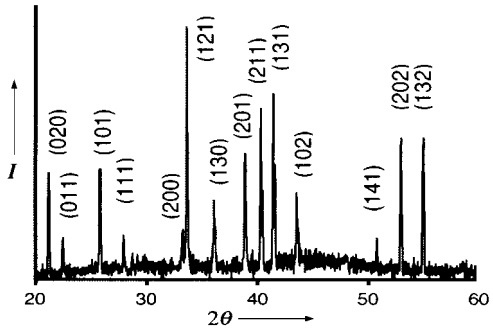

Figure 3. XRD pattern displaying the formation of orthorhombic $Mg_3B_2O_6$ on a Si wafer. $I=$ intensity (arbitrary units).

The nanotubes were further characterized by a high-resolution transmission electron microscope (HRTEM). Figure 4 a depicts a typical individual nanotube with a width of about 400 nm. The microanalysis of the chemical composition by energy dispersive spectrometry (EDS) and electron energy loss spectrometry (EELS) demonstrated that the tube is composed of B, O, and Mg. A typical EDS spectrum is shown in the inset of Figure 4 a. Both the quantitative analyses from EELS and EDS gave an approximate Mg:B:O atomic ratio of 1.0:0.6:2.0, which is very close to the elemental composition in $Mg_3B_2O_6$. Selected area electron diffraction (ED) patterns were also recorded by tilting the nanotube to different zone axes during transmission electron microscopic (TEM) obser-

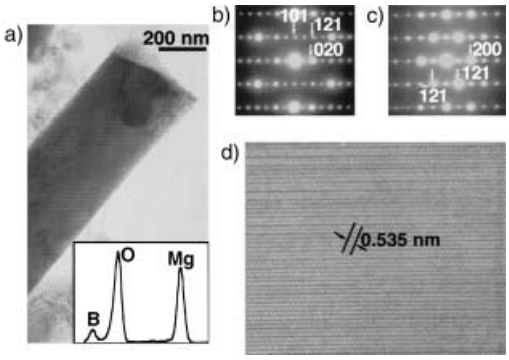

Figure 4. TEM verification of the orthorhombic $Mg_3B_2O_6$ structure of these nanotubes. a) TEM image of an individual nanotube, the inset is a EDS spectrum that shows the tube is composed of B, O and Mg atoms; b),c) ED patterns recorded along the $[10\bar{1}]$ and $[01\bar{2}]$ zone axes, respectively; d) HRTEM image corresponding to the ED pattern in (c). An interplanar spacing of the (121) lattice planes is indicated.

vations (Figure 4b,c). The ED pattern in Figure 4b can be indexed as that of the single crystalline orthorhombic $Mg_3B_2O_6$ recorded along the $[10\bar{1}]$ zone axis. Similarly, the ED pattern (Figure 4c) agrees well with the $[01\bar{2}]$ reflections of $Mg_3B_2O_6$. Figure 4d depicts the HRTEM image corresponding to the ED pattern in Figure 4c. In general, the ED patterns of the nanotubes are similar to those of bulk $Mg_3B_2O_6$. We have, however, measured an *a* axis expansion of about 3% in the nanotubes. This difference may be ascribed to the geometrical effects of the tubelike structures although it is not clear why only the *a* axis is influenced.

We consider that the formation of magnesium borate nanotubes is initiated through the oxidization of the boron film on the Si wafer, and the simultaneous vaporization and deposition of Mg chips. At elevated temperature (ca. 850 °C), the amorphous B nanoparticles are oxidized to form molten B_2O_3 layers on their surfaces. Subsequently a polymeric vitreous $(BO)_n$ complex may be formed through the reaction between dissolved boron and molten B_2O_3. Simultaneously, Mg chips, laid below the Si wafer (500–550 °C), are also vaporized or oxidized. The Mg or MgO vapors deposit onto the vitreous B_2O_3 or $(BO)_n$ layer on the Si surface. This process continues until the supersaturation level of Mg species is reached in the vitreous layer, and precipitation of the magnesium borate species occurs. This initiates the 2D nuclei sites of the nanotubes as shown in Figure 2. The subsequent nanotube growth from these nuclei voids may proceed through the continual precipitation of magnesium borates, while the voids form hollow cores. The growth may be promoted by the temperature gradient normal to the Si wafer due to the IR irradiation heating from the top surface. This growth scenario is quite different from that of the more ubiquitous layered compounds (such as C, BN and MoS_2), which consist of a hexagonal or trigonal lattice that forms nanotubes by the spiral winding of molecular layers.[1,2,3b] Detailed structural modeling and computing are needed to reveal how nanotubes could be formed in magnesium borates.

The supersaturation of Mg or MgO and the precipitation of magnesium borate species strongly depend on the partial concentrations of Mg or MgO in the vitreous layer. Because of the low melting point of Mg (ca. 650 °C), the vaporization or oxidization of Mg chips may be more dominant in the surrounding environment. It is therefore reasonable to deduce that the vitreous B_2O_3 or $(BO)_n$ layer is sufficient, or abundant with respect to MgO. According to the phase diagram of MgO–B_2O_3, $Mg_3B_2O_6$ is more likely to form when MgO is enriched.[10] This observation may explain the formation of nanotubes of $Mg_3B_2O_6$ ($3MgO{\cdot}B_2O_3$) rather than MgB_4O_7 ($MgO{\cdot}B_2O_3$) or $Mg_2B_2O_5$ ($2MgO{\cdot}B_2O_3$).

In summary, $Mg_3B_2O_6$ nanotubes were successfully synthesized by heating a boron thin film with IR radiation in the presence of Mg vapor and traces of oxygen. As demonstrated by this successful example, this technique may be easily modified or extended to prepare nanotubes of other metal borates. It therefore has an outstanding potential in providing customized nanotubes for a broad range of nanotechnology applications.

Experimental Section

The experiments were carried out in an IR-irradiation-heating furnace. Amorphous boron powders (99.9%, ca. 50 nm) and Mg chips (99.5%), purchased from WAKO Pure Chemical Industries, were used as received. A Si (001) wafer (25.4 mm in diameter) was used as the heating target. First, boron powders were dispersed in acetone by ultrasound, then dripped onto the Si (001) mirror-polished surface to form a thin film. The Si wafer was then placed on a BN holder with the boron film downwards, which acted as a deposition substrate. Mg chips were laid under the Si wafer with a 2 mm distance between the boron film and Mg chips. When the chamber was evacuated (< 5 Torr), a gas flow of Ar (500 mL min^{-1}) and O_2 (10 mL min^{-1}) was introduced. The Si wafer was rapidly heated to 850 °C by IR irradiation of the top Si surface. The temperature of the Mg chips under the Si wafer was estimated to be 500–550 °C during the heating process. The heating process generally continued for approximately 30 minutes. The chamber was then cooled to room temperature and the Si wafer was removed for thorough characterization. A small piece of Si was cleaved from a larger wafer and directly observed by SEM. The structural and chemical natures of the nanotubes were studied using HRTEM equipped with EDS and EELS. A TEM sample was prepared by stripping a small piece of the film from the Si wafer, which was dispersed by ultrasound in acetone, then transferred onto a carbon coated copper grid. All TEM images and diffraction patterns were taken using a JEM-3000F field emission microscope operated at 300 keV.

Received: October 29, 2002
Revised: December 18, 2003 [Z50455]

Keywords: borates · crystal growth · nanostructures · nanotubes

[1] S. Iijima, *Nature* **1991**, *354*, 56.
[2] N. G. Chopra, R. J. Luyken, K. Cherrey, V. H. Crespi, M. L. Cohen, S. G. Louie, A. Zettl, *Science* **1995**, *269*, 966.
[3] a) R. Tenne, L. Margulis, M. Genut, G. Hodes, *Nature* **1992**, *360*, 444; b) Y. Feldman, E. Wasserman, D. J. Srolovitz, R. Tenne, *Science* **1995**, *267*, 222; c) L. M. Rendina, R. J. Puddephatt, *Chem. Rev.* **1997**, *97*, 1735; d) Y. R. Hacohen, E. Grunbaum, R. Tenne, J. Sloan, J. L. Hutchison, *Nature* **1998**, *395*, 336; e) M. Nath, C. N. R. Rao, *J. Am. Chem. Soc.* **2001**, *123*, 4841; f) M. Nath, C. N. R. Rao, *Angew. Chem.* **2002**, *114*, 3601; *Angew. Chem. Int. Ed.* **2002**, *41*, 3451; g) Y. R. Hacohen, E. Grunbaum, R. Tenne, J. Sloan, J. L. Hutchison, *Nature* **1998**, *395*, 336.
[4] a) M. E. Spahr, P. Bitterli, R. Nesper, M. Muller, F. Krumeich, H. U. Nissen, *Angew. Chem.* **1998**, *110*, 1339; *Angew. Chem. Int. Ed.* **1998**, *37*, 1263; b) T. Kasuga, M. Hiramatsu, A. Hoson, T. Sekino, Niihara, K. *Langmuir* **1998**, 14, 3160; c) Y. Li, Y. Bando, *Chem. Phys. Lett.* **2002**, *364*, 484.
[5] a) M. R. Ghadirl, J. R. Granja, R. A. Milligan, D. E. McRee, N. Khazanovich, *Nature* **1993**, *366*, 324; b) M. R. Ghadirl, J. R. Granja, L. K. Buehler, *Nature* **1994**, *369*, 301; c) M. Steinhart, J. H. Wendorff, A. Greiner, R. B. Wehrspohn, K. Nielsch, J. Schilling, J. Choi, U. Gosele, *Science* **2002**, *296*, 1997.
[6] R. Ma, Y. Bando, T. Sato, C. Tang, F. Xu, *J. Am. Chem. Soc.* **2002**, *124*, 10668.
[7] a) M. Prockic, *Nucl. Instrum. Methods* **1980**, *175*, 83; b) D. I. Shahare, S. J. Dhoble, S. V. Moharil, *J. Mater. Sci. Lett.* **1993**, *12*, 1873.
[8] Z. S. Hu, R. Lai, F. Lou, L. G. Wang, Z. L. Chen, G. X. Chen, J. X. Dong, *Wear* **2002**, 252, 370.
[9] H. McMurdie, M. Morris, E. Evans, B. Paretzkin, W. Wong-Ng, Y. Zhang, *Powder Diffr.* **1987**, *2*, 47.
[10] T. Mutluer, M. Timucin, *J. Am. Ceram. Soc.* **1975**, *58*, 196.

